Scientific Voyage
Vol. 2, No. 3,
Page 1-8 (2021)

SCIENTIFIC VOYAGE
ISSN: 2395-5546

GCECT
Publication
July - Sept.

Silver Nanoparticles: potential and promising means to combat pathogenic microorganisms

Rini Roy [a1] and Aditi Nag Chaudhuri [b2]

[a] *Post Graduate Department of Microbiology, Bidhannagar College, Kolkata, W.B., India*

[b] *Post Graduate Department of Microbiology, Lady Brabourne College, Kolkata, W.B., India*

Abstract: Nanotechnology is a rapidly expanding field with its applications in biomedical sciences and is associated with the engineering and production of materials at the atomic and molecular level. Study of silver nanoparticles has a wide application in various fields. Metal nanoparticles are the most promising due to their anti-bacterial properties which, occurs because of the high surface to volume ratio. Silver nanoparticles (AgNPs) are particularly excellent because of their potential applications in health care, textile fibers, food packaging, and antibacterial fields. When used in relatively low concentrations at the same size and shape Ag-NPs are non-toxic or less harmful to mammalian tissues and environmentally friendly. In this study an overview on the synthesis of AgNPs from different sources and their antibacterial activity has been given. The physical and chemical methods and green synthesis as well as microbial synthesis of AgNPs are mentioned here. It has been shown that synergistic action of AgNPs and antibiotics have antibacterial effect on pathogenic bacteria [1].

Keywords: silver nanoparticles; pathogenic bacteria; reducing agents; antibiotics

1 Introduction

Nanotechnology is a significant research field which deals with particle structures ranging from approximately 1-100 nm as also their design, synthesis, and manipulation. Nanobiotechnology is a multidisciplinary aspect where nanoparticles used in biological systems encompasses the disciplines of biology, biochemistry, chemistry, engineering, physics and medicine. Moreover, the nanobiotechnology also involves clean, nontoxic, and eco-friendly procedures for the synthesis of metal NPs having the intrinsic ability to reduce metals by specific metabolic pathways [2-7]. Green synthesis approaches include mixed valence polyoxometalates, polysaccharides, Tollens, biological, and irradiation method which renders less environmental toxicity. Solvent medium selection and selection of eco-friendly nontoxic reducing and stabilizing agents are the main criteria in green synthesis of NPs [8].

The importance of silver NPs results from the unique properties which can be incorporated into antimicrobial applications, biosensor materials, composite fibers, cryogenic super-conducting materials, cosmetic products, and electronic components. Some important applications of silver NPs are in pharmaceutics, medicine, and dentistry. There are many physical and chemical methods used for synthesizing and stabilizing silver NPs.

Silver nanoparticle based antibacterial agents are the need of the hour in the present scenario of multidrug resistance in microorganisms. The antibacterial mechanisms of silver nanoparticles are dependent on different structural factors including surface chemistry, size, and shape [9]. Silver is least toxic among other elements with respect to oligodynamic effect against microorganisms. So, silver-based materials like silver nanoparticles are useful exhibiting antimicrobial properties by damaging not only the key enzymes in the pathogenic bacterial cell membranes but also by penetrating the bacteria [10].

---

[1] Email: for_rini_roy@yahoo.co.in
[2] Email: odditybiom@gmail.com

Silver nanoparticles (AgNps) have been found to be effective in case of hospital isolated *Pseudomonas aeruginosa* which is generally considered as a multidrug resistant strain [11].

2 Preparation of silver nanoparticles

2.1 Physical methods

Evaporation-condensation and laser ablation are the most important physical methods for the preparation of AgNPs. The advantages of physical synthesis methods in comparison with chemical processes are the absence of solvent contamination in the prepared thin films and the uniformity of NPs distribution.

A small ceramic heater with a local heating area has been used to synthesize AgNPs [12]. To evaporate source materials the small ceramic heater was used. The evaporated vapor can cool at a suitable rapid rate since the temperature gradient in the vicinity of the heater surface is very steep compared to that of a tube furnace.

The formation of small NPs in high concentration results from this method. As the fluctuation of temperature of the heater surface does not take place with time the particle generation is very stable This physical method can be used for two purposes - as a nanoparticle generator for long-term experiments for inhalation toxicity studies, and as a calibration device for nanoparticle measurement equipment [12].

Laser ablation of metallic bulk materials in solution is a technique by which silver NPs could be synthesized [13]. The wavelength of the laser impinging the metallic target, the duration of the laser pulses (in the femto-, pico- and nanosecond order), the laser fluence, the ablation time duration and the effective liquid medium, with or without the presence of surfactants are the parameters on which the ablation efficiency and the characteristics of produced nano-silver particles depend [14].

One important advantage of laser ablation technique in comparison with other methods for production of metal colloids is the absence of chemical reagents in solutions.

Tien and co-workers [15] used the arc discharge method to synthesize silver NPs suspension in deionized water with no added surfactants. In this method, silver wires (Gredmann, 99.99%, 1 mm in diameter) were submerged in deionized water and used as electrodes. With a silver rod consumption rate of 100 mg/min, yielding metallic silver NPs of 10 nm in size, and ionic silver obtained at concentrations of approximately 11 ppm and 19 ppm, respectively.

The synthesis of silver NPs by direct metal sputtering into the liquidmedium was shown by Siegel and colleagues [16]. An interesting alternative to time-consuming, wet-based chemical synthesis techniques is the method combining physical deposition of metal into propane-1,2,3-triol (glycerol).

2.2 Chemical methods: Chemical reduction

The chemical reduction by organic and inorganic reducing agents is the most common approach for synthesis of AgNPs. Different reducing agents have been used in aqueous or non-aqueous solutions, leading to formation of metallic silver (Ag), which is followed by assembly into nanoparticles. These different reducing agents include sodium citrate, ascorbate, sodium borohydride (NaBH4), elemental hydrogen, polyol process, Tollens reagent, N, N-dimethylformamide (DMF), and poly (ethylene glycol)-block copolymers. Reduction of Ag^{+} to metallic silver (Ag^{0}) by these reducing agents is followed by agglomeration into oligomeric clusters which eventually lead to the formation

of metallic colloidal silver particles [17]. Some protective agents are used to stabilize dispersive NPs during metal nanoparticle preparation and protect the NPs that can be absorbed on or bind onto nanoparticle surfaces, avoiding their agglomeration [18]. The presence of surfactants consisting functional groups like thiols, amines, acids, and alcohols are responsible for interactions with particle surfaces which can stabilize particle growth. Thus, these surfactants protect particles from sedimentation, agglomeration, or losing their surface properties.

Polymeric compounds such as poly (vinyl alcohol), poly (vinylpyrrolidone), poly (ethylene glycol), poly (methacrylic acid), and polymethylmethacrylate have been found to be the effective protective agents to stabilize NPs. Oliveira and co-workers[18] in one study prepared dodecanethiol-capped silver NPs based on Brust procedure [19]where a phase transfer of an Au^{3+} complex from aqueous to organic phase in a two-phase liquid-liquid system occurred, which was followed by a reduction with sodium borohydride in the presence of dodecanethiol as stabilizing agent. Dodecanethiol binding onto the NPs surfaces, avoided their aggregation and made them soluble in certain solvents. Dramatic modifications in nanoparticle structure, average size, size distribution width, stability and self-assembly patterns were observed due to small changes in synthetic factors. Kim and colleagues [20] showed production of spherical silver NPs with a controllable size and high monodispersity using the polyol process and a modified precursor injection technique. The injection rate and reaction temperature were important factors for producing uniform-sized silver NPs with a reduced size in the precursor injection method.

In the process of preparation of AgNPs at room temperature, the corresponding metal ions are mixed with reduced polyoxometalates which serves as reducing and stabilizing agents. Polyoxometalates are soluble in water. They have the capability of undergoing stepwise, multielectron redox reactions without disturbing their structure. It was shown that AgNPs were produced by illuminating a deaerated solution of polyoxometalate/S/Ag^{+} [21]. It has been reported that green chemistry-type one-step synthesis and stabilization of silver nanostructures with MoV–MoVI mixed-valence polyoxometalates occur in water at room temperature [22].

2.3 Microemulsion techniques

Microemulsion techniques are used to synthesize uniform and size controllable AgNPs.The initial spatial separation of reactants (metal precursor and reducing agent) in two immiscible phases is the basis for the NPs preparation in two-phase aqueous organic systems. A quaternary alkyl-ammonium salt mediates the interface between the two liquids and the intensity of inter-phase transport between two phases. This affects the rate of interactions between metal precursors and reducing agents. Due to surface coating with stabilizer molecules occurring in the non-polar aqueous medium metal clusters formed at the interface are stabilized and transferred to the organic medium by the inter-phase transporter [23]. The use of highly deleterious organic solvents is one of the major disadvantages.

Thus, separation and removal of large amounts of surfactant and organic solvent from the final product is necessary. Use of dodecane by Zhang and co-workers [24] as oily phase (a low deleterious and even nontoxic solvent), reduced the necessity to separate the prepared silver solution from the reaction mixture. Colloidal NPs prepared in nonaqueous media for conductive inks are well-dispersed in a low vapor pressure organic solvent which readily wet the surface of polymeric substrate without any aggregation. Metal nanoparticles are applied as catalysts to catalyse most organic reactions being conducted in non-polar solvents. Transferring metal NPs to different physicochemical environments are important in practical applications [25].

2.4 UV-initiated photoreduction

UV-initiated photoreduction is a simple and effective method for synthesis of silver NPs in the presence of citrate, polyvinylpyrrolidone, poly (acrylic acid), and collagen. Silver NPs produced by Huang and Yang via photoreduction of silver nitrate in layered inorganic laponite clay suspensions served as stabilizing agent for prevention of NPs aggregation. The properties of produced NPs are expressed as a function of UV irradiation time. When irradiated under UV for 3 h, bimodal size distribution and relatively large silver NPs were obtained. The silver NPs disintegrated into smaller sizes with a single distribution mode on further irradiation. This disintegration continued until a relatively stable size and size distribution was obtained [26]. Poly (vinyl alcohol) served as protecting and stabilizing agent for preparation of the Silver NPs (nanosphere, nanowire, and dendrite) by UV irradiation photo reduction technique at room temperature. Significant contribution in the growth of the nanorods and dendrites depended on concentration of both poly (vinyl alcohol) and silver nitrate [27].

2.5 Photoinduced reduction

Photoinduced or photocatalytic reduction methods can be used to synthesize silver NPs because this process has high spatial resolution, convenience of use, and great versatility. Photochemical synthesis can design the NPs in various mediums including cells, emulsion, polymer films, surfactant micelles, glasses, etc. Poly (styrene sulfonate)/poly (allylamine hydrochloride) polyelectrolyte capsules are used as microreactors for preparing Nano-sized silver particles with an average size of 8 nm by photoinduced reduction [28]. Photoinduced method converts silver nanospheres into triangular silver nanocrystals (nanoprisms) with desired edge lengths in 30-120 nm range [29]. Particle growth process was regulated using dual-beam illumination of NPs. Citrate and poly (styrene sulfonate) act as stabilizing agents in this process.

In the presence of sodium citrate (NaCit), the direct photo-reduction process of $AgNO_3$ was conducted with different light sources (UV, white, blue, cyan, green and orange) at room temperature. This light-modification process results in a colloid with distinctive optical properties relating to the size and shape of the particles [30]. UV photo-activation method has been used for the preparing stable silver NPs in aqueous Triton X-100 (TX-100)[31]. TX-100 molecules serve dual role of reducing agent and of NPs stabilizer through template/capping action.

Furthermore, surfactant solution by decreasing the diffusion or mass transfer co-efficient of the system carry out the process of NPs growth in the diffusion-controlled way. It governs NPs size distributions by increasing the surface tension at the solvent-NPs interface.

2.6 Irradiation methods

Silver NPs with a well-defined shape and size distribution are obtained by laser irradiation of an aqueous solution of silver salt and surfactant [32]. Use of laser in a photo-sensitization synthetic method of making silver NPs required benzophenone. Low laser powers produced silver NPs of about 20 nm, but an increased irradiation power synthesized NPs of about 5 nm. Light sources used for production of silver NPs were laser and mercury lamp [33]. Photo-sensitized growth of silver NPs using thiophene (sensitizing dye) was observed in visible light irradiation studies and by illumination of $Ag(NH3)^+$ in ethanol silver nanoparticle formation has been done [34, 35].

2.7 Microwave-assisted synthesis

Microwave-assisted synthesis is a method which is worthy to mention for synthesis of AgNPs. For consistently yielding nanostructures with smaller sizes, narrower size distributions, and a higher degree of crystallization microwave heating is better than a conventional oil bath [36]. The

advantages of microwave heating are shorter reaction times, reduced energy consumption, and better product yields preventing the agglomeration of the particles formed [36].

Using carboxymethyl cellulose sodium as reducing and stabilizing agent AgNPs could be synthesized by microwave-assisted synthesis method. Concentration of sodium carboxymethyl cellulose and silver nitrate control the size of AgNPs. The produced AgNPs remained uniform and stable at room temperature for 2 months without any visible changes [37]. Pt seeds, polyvinyl pyrrolidine and ethylene glycol help in the synthesis of AgNPs [38].

2.8 Green synthesis

Metal nanoparticles produced by Green synthesis of using various plants like extracts of *Cacumen platycladi*, *Eucalyptus citriodora* and *Ficus bengalensis, Ocimum sanctum* leaf and plant products has recently been successfully accomplished. The AgNPs synthesized from these plants or plant parts are shown to show the antimicrobial activities against pathogenic microorganisms [39-41].

2.9 Microbial synthesis

Waste material from the corn industry has been utilised for the synthesis of silver nanoparticles to demonstrate the antibacterial activities against food borne pathogens like *Bacillus cereus* ATCC 13061, *Staphylococcus aureus* ATCC 49444, *Listeria monocytogenes* ATCC 19115, *Escherichia coli* ATCC 43890, and *Salmonella Typhimurium* ATCC 43174. Microorganisms are also able to synthesize AgNPs. The characterization of biosynthesized AgNPs were done by UV-Vis spectrophotometry along with surface plasmon resonance at 450 nm as also by using scanning electron microscope, X-ray diffraction, Fourier-transform infrared spectroscopy and thermogravimetric analysis [42].

The shape and size of the resulting AgNPs largely depended on experimental parameters like temperature, concentration of the Ag(I) compound, pH solution. In the case of biological synthesis, the shape and size are depended on the direct object used to produce AgNPs [43].

3 Mode of action of AgNPs on cells

There are different mechanisms by which AgNPs exert its antibacterial effect/ adhesion on the surface of the bacterial cell wall and membrane. The mode of penetration into the cell and disruption of intracellular organelles and biomolecules, induction of oxidative stress, and modulation of signal transduction pathways have been studied for AgNps[44]. On the cell surface for Gram-negative bacteria the adhesion and accumulation of AgNPs takes place. There are water-filled channels called porins in the outer membrane of Gram-negative bacteria through which AgNPs can penetrate bacterial cells. Passive transport of hydrophilic molecules of various sizes and charges across the membrane occurs through porins. The thicker cell wall of Gram-positive bacteria is responsible for the penetration of silver ions into the cytoplasm, therefore the effect of AgNPs is more pronounced in Gram-negative bacteria than in Gram-positive bacteria. The presence of lipopolysaccharides attributes to the structural integrity of the Gram-negative bacteria cell wall, making such bacteria more sensitive to silver nanoparticles because the negative charge of the lipopolysaccharides promotes AgNP adhesion. It has been predicted that the ability of silver nanoparticles to attach to the bacterial cell wall is due to the electrostatic interaction between positively charged silver ions and the negatively charged surface of the cell membrane due to the carboxyl, phosphate, and amino groups, give an

opportunity to subsequently penetrate it, thereby causing structural changes in the cell membrane and, as a result, its permeability [45].

Thus, proton motive force (PMF) is dissipated and then membrane is destroyed. AgNPs may also act as a carrier to transport Ag^+ more efficiently to bacterial cells whose proton motive force would consequently reduce the local pH and increase Ag^+ release. Silver nanoparticles damage the cell membrane by forming free radicals upon contact with bacteria thus making it porous. However, in the view of others AgNPs adhere to the surface of bacteria and change the membrane properties, while inside the bacterial cell, they can lead to DNA damage.

Inhibition of transcription occurs due to the penetration of AgNPs into the cell where they could associate with intracellular elements such as lipids, proteins and DNA [45].

4 Applications of AgNPs

Due to antibacterial, antifungal, antiviral, larvicidal, antiplasmodial, anthelmintic and leishmanicidal activity AgNPs have versatile applications [45].

AgNPs have their application in dental medicine, cardiology and dermatology by virtue of their antimicrobial activity [46].

The smaller the particle size of Ag-NPs, the smaller the value of the minimum inhibitory concentration (MIC) and minimum bactericidal concentrations (MBC), indicating the greater the antibacterial activity [47].

The aqueous extract of *Murraya koenigii* leaves was used for synthesis of silver nanoparticlesand their antibacterial potential was evaluated on multiple Extended-spectrum β-lactamase (ESβL) producing genteric bacteria and Methicillin Resistant *Staphylococcus aureus* (MRSA). The AgNps prepared from plant extract inhibited the growth of the test pathogens on nutrient agar plates with varying zones of inhibition [48].

Rapid synthesis of silver nanoparticles can be done by the combination of culture supernatant of bacteria. The AgNP synthesized from *S.aureus* was tested for antimicrobial activity by well diffusion method, against pathogenic organisms such as MRSA, MRSE, *Streptococcus pyogenes, Salmonella typhi*, *Klebsiella pneumoniae* and *Vibrio cholorae*. The zone of inhibition was observed [49].

There are different studies which revealed that the plant and fungus can also produce silver nanoparticles. Using *Penicillium purpurogennum* silver nanoparticles have been successfully produced [50]. They found that increase in concentration of silver nitrate solution increases the formation of silver nanoparticles. They have also reported that, the change in pH of the reaction mixture led to the change in the shape and size of the silver nanoparticles [49].

In our study [1] the purpose was to prepare different silver nanoparticles and to observe the antimicrobial effect of only the silver nanoparticles on pathogenic microorganisms like *E. coli*, *Salmonella* sp., *Vibrio cholera* isolated from the water samples collected from the East Kolkata Wetland. In our studies experiments were designed to observe the antimicrobial effect of silver nanoparticles along with different types of chemicals (SDS, lysozyme) on pathogenic microorganisms and to observe the antimicrobial effect of silver nanoparticles along with different types of antibiotics like Ampicillin, Streptomycin, Tetracycline, Chloramphenicol, Gentamycin, Erythromycin and Kannamycin on pathogenic microorganisms.

5 Conclusion

The silver nanoparticles prepared with various reducing agents in our study were found to be effective antimicrobial agent, effective against pathogenic bacteria. The silver nanoparticle prepared along with sodium citrate was found to be highly effective in retarding the growth of pathogenic bacteria in comparison to the AgNPs prepared with sodium borohydride and that prepared with pyrogallol [1]. When AgNPs prepared with sodium citrate was used along with SDS, it effectively reduced the size of the pathogenic bacteria and retarded their growth.

When AgNPs prepared with sodium citrate was used along with antibiotic ampicillin, it was seen that *E. coli* cells which were ampicillin resistant turned out to be ampicillin sensitive strains [1]. A possible cause for this phenomenon could be that the silver nanoparticle helped in the entry of ampicillin inside the cells, or it can also be that the silver nanoparticle helped to destroy the thiol (–SH) of beta lactamase thus turning the ampicillin resistant strains to ampicillin sensitive strains.

The prepared silver nanoparticles can thus be effectively used as antimicrobial agents along with antibiotics and the different structures may attribute to their different mode of action. As AgNPs are cheap and have low cytotoxicity, so they can be used as an alternative antimicrobial agent.

References

1. R. Roy, A. Pal and A.N. Chaudhuri, *Int. J. Appl. Res.* **1** (2015) 745.

2. V.L. Colvin, M.C. Schlamp and A. Alivisatos, *Nature*, **370** (1994) 354.

3. Y. Wang and N. Herron, *J. Phys. Chem.* **95** (1991) 525.

4. G. Schmid, *Chem. Rev.* **92** (1992) 1709.

5. A.J. Hoffman, G. Mills, H. Yee and M. Hoffmann, *J. Phys. Chem.* **96** (1992) 5546.

6. J.F. Hamilton and R. Baetzold, *Science* **205** (1979) 1213.

7. H.S. Mansur, F. Grieser, M. S. Marychurch, S. Biggs, R.S. Urquhart and D. Furlong, *J. Chem. Soc. Faraday Trans.* **91** (1995) 665.

8. S. Iravani, H. Korbekandi, S.V. Mirmohammadi and B. Zolfaghari, *Res. Pharma. Sci.* **9** (2014) 385.

9. S. Tang and J. Zheng, *Adv. Healthcare Mat.* **7** (2018) 1701503.

10. I.T. Nzekwe, C.O. Agubata, C.E. Umeyor, I.E. Okoye and C.B. Ogwueleka, *British J. Pharma. Res.* **14** (2016) 1.

11. Y.Y. Loo, Y. Rukayadi, M. A. R. Nor-Khaizura, C.H. Kuan, B.W. Chieng, M. Nishibuchi and S. Radu, *Front. Microbio.* **9** (2018) 1.

12. J. Jung, H. Oh, H. Noh, J. Ji and S. Kim, *J. Aerosol Sci.* **37** (2006) 662.

13. S.I. Dolgaev, A.V. Simakin, V.V. Voronov, G.A. Shafeev and F. Bozon-Verduraz, *Appl. Surf. Sci.* **186** (2002) 546.

14. M. Kawasaki and N. Nishimura, *Appl. Surf. Sci.* **253** (2006) 2208.

15. D.-C. Tien, K.-H. Tseng, C.-Y. Liao, J.-C. Huang and T.T. Tsung, *J. Allo. Comp.* **463** (2008) 408.

16. J. Siegel, O. Kvítek, P. Ulbrich, Z. Kolská, P. Slepička and V. Švorčík, *Mater. Lett.* **89** (2012) 47.

17. G. Merga, R. Wilson, G. Lynn, B. Milosavljevic and D. Meisel, *J. Phys. Chem. C* **111** (2007) 12220.

18. M. Oliveira, D. Ugarte, D. Zanchet, A. Zarbin, *J. Colloid Interf. Sci.* **292** (2005) 429.

19. M. Brust, C. Kiely, *Phys. Eng. Aspects* **202** (2002) 175.

20. D. Kim, S. Jeong and J. Moon, *Nanotech.* **17** (2006) 4019.

21. A. Troupis, A. Hiskia, E. Papaconstantinou, *Angew Chem. Int. Ed.* **41** (2002) 1911.

22. G. Zhang, B. Keita, A. Dolbecq, P. Mialane, F. Secheresse and F. Miserque, *Chem. Mater.* **19** (2007) 5821.

23. Y. Krutyakov, A. Olenin, A. Kudrinskii, P. Dzhurik and G. Lisichkin, *Nanotech. Russia* **3** (2008) 303.

24. W. Zhang, X. Qiao and J. Chen, *Physicochem. Eng. Aspects* **299** (2007) 22.

25. P. Cozzoli, R. Comparelli, E. Fanizza, M. Curri, A. Agostiano and D. Laub, *J. Am. Chem. Soc.* **126** (2004) 3868.

26. H. Huang and Y. Yang, *Compos. Sci. Technol.* **68** (2008) 2948.

27. Y. Zhou, S.H. Yu, C.Y. Wang, X.G. Li, Y.R. Zhu and Z.Y. Chen, *Adv. Mater.* **11** (1999) 850.

28. D.G. Shchukin, I.L. Radtchenko and G. Sukhorukov, *Chem. Phys. Chem.* **4** (2003) 1101.

29. R. Jin, Y.C. Cao, E. Hao, G.S. Metraux, G.C. Schatz and C. Mirkin, *Nature* **425** (2003) 487.

30. R. Sato-Berrú, R. Redón, A. Vázquez-Olmos and J. Saniger, *J. Raman Spectros.* **40** (2009) 376.

31. S.K. Ghosh, S. Kundu, M. Mandal, S. Nath and T. Pal, *J. Nanopart. Res.* **5** (2003) 577.

32. J.P. Abid, A.W. Wark, P.F. Brevet and H.H. Girault, *Chem. Commun.* **7** (2002) 792.

33. S. Eutis, G. Krylova, A. Eremenko, N. Smirnova, A.W. Schill, M. El-Sayed, *Photochem. Photobiol. Sci.* **4** (2005) 154.

34. P. K. Sudeep and P.V. Kamat, *Chem. Mater.* **17** (2005) 5404.

35. L. Zhang, J.C. Yu, H.Y. Yip, Q. Li, K.W. Kwong and A.-W. Xu, *Langmuir.* **19** (2003) 10372.

36. M.N. Nadagouda, T.F. Speth and R. Varma, *Acc. Chem. Res.* **44** (2011) 469.

37. J. Chen, K. Wang, J. Xin and Y. Jin, *Mater. Chem. Phys.* **108** (2008) 421.

38. S. Navaladian, B. Viswanathan, T.K. Varadarajan and R.P. Viswanath, *Nanotech.* **19** (2008) 045603.

39. S. Ravindra, Y.M. Mohan, N.N. Reddy and K.M. Raju, *Physicochem. Eng. Aspects.* **367** (2010) 31.

40. G. Singhal, R. Bhavesh, K. Kasariya, A.R. Sharma and R.P. Singh, *J. Nanopart. Res.* **13** (2011) 2981.

41. M. Sathishkumar, K. Sneha, S.W. Won, C.-W. Cho, S. Kim and Y.S. Yun, *Biointerf.* **73** (2009) 332.

42. J.K. Patra and K.H. Baek, *Front. Microbiol.* **8** (2017) 1.

43. O.V. Mikhailov and E.O. Mikhailova, *Materials* **12** (2019) 3177.

44. T.C. Dakal, A. Kumar, R.S. Majumdar and V. Yadav, *Front. Microbiol.* **7** (2016) 1831.

45. E. katerina and O. Mikhailova, *J. Funct. Biomater*. **11** (2020) 1.

46. J. Talapko, T. Matijevi´c, M. Juzbaši´c, A. Antolovi´c-Požgain and I. Škrlec, *Microorgan.* **8** (2020) 1.

47. Y. Dong, H. Zhu, Y. Shen, W. Zhang and L. Zhang, *Plos One* **14** (2019) 1.

48. F.A. Qais, A. Shafiq, H.M. Khan, F.M. Husain, R.A. Khan, B. Alenazi, A. Alsalme and I. Ahmad, *Hindawi Bioinorganic Chemistry and Applications* **2019** (2019) 4849506.

49. K.V. Selvi and T. Sivakumar, *Int. J. Adv. Res. Bio. Sci.* **3** (2016) 292.

50. R.R. Nayak, N. Pradhan, D. Behera, K.M. Pradhan, S. Mishra, L.B. Sukla and B.K. Mishra, *J. Nanopart. Res.* **13** (2011) 3129.

Scientific Voyage
Vol. 2, No. 3,
Page 9-20 (2021)

SCIENTIFIC VOYAGE
ISSN: 2395-5546

GCECT
Publication
July - Sept.

Accelerating universe and anisotropic dark energy models

S.K. Tripathy[a1], A. Anand[b], Asmita Parida[c], B. Mishra[d2] and Saibal Ray[e3]

[a] *Department of Physics, Indira Gandhi Institute of Technology, Sarang, Dhenkanal 759146, Odisha, India*
[b] *Department of Computer Science Engineering and Applications, Indira Gandhi Institute of Technology, Sarang, Dhenkanal 759146, Odisha, India*
[c] *Department of Electrical Engineering, Indira Gandhi Institute of Technology, Sarang, Dhenkanal 759146, Odisha, India*
[d] *Department of Mathematics, Birla Institute of Technology and Science-Pilani, Hyderabad Campus, Hyderabad 500078, India*
[e] *Department of Physics, Government College of Engineering and Ceramic Technology, Kolkata 700010, West Bengal, India*

Abstract: We discussed some accelerating anisotropic dark energy models with dynamic pressure anisotropies along different spatial directions in the framework of General Relativity. A spatially homogeneous but anisotropic LRSBI space time is considered to model the universe. Explicit expressions for directional pressure anisotropies are obtained in terms of the deceleration parameter. This provides us an opportunity to tune the evolutionary aspect of the pressure anisotropies through the evolving nature of the deceleration parameter. It is found that, for models predicting constant deceleration parameter, the pressure anisotropies are maintained throughout the cosmic evolution. However, for models simulating a signature flipping deceleration parameter, the pressure anisotropies along the symmetry axis and symmetry plane are found to evolve dynamically and continue along with the cosmic expansion.

Keywords: general relativity; dark energy; anisotropy; hybrid scale factor; cosmology

1 Introduction

The most striking and intriguing aspect of modern cosmological theories is to explain the outcome of a lot of observational data gathered over the last two decades suggesting an accelerated expansion of the universe at least at its late phase of evolution [1,2]. Also, there have been observational supporting evidences on the belief that, the expansion rate based on local data is different than the past expansion rate [3]. Lot of theoretical explanations and concepts have been developed so far to address this late time cosmic speed up issue. Also, these developments have raised many questions and doubts. Einstein's General Relativity (GR) is unable to provide suitable answers to these questions concerning the cosmic acceleration at late phase. Therefore, a negligibly small but positive cosmological constant is put by hand in the field equations of GR to get a possible accelerating scenario. However,

[1] Email: tripathy_ sunil@rediffmail.com
[2] Email: bivu@hyderabad.bits-pilani.ac.in
[3] Email: saibal@associates.iucaa.in

within the purview of GR, it is believed that the dark sector of the universe is responsible for the ongoing cosmic dynamics. The dark sector is comprising of the dark matter and the dark energy. The dark energy is believed to have played a role in the late time accelerating dynamics. The dark energy still remains as a mystery besides the known fact that, it violates the strong energy condition and resembles a cosmic fluid with negative pressure. On the other hand, the dark matter is believed to be controlled by a weakly interacting massive particle (WIMP) [4,5]. There are also views on the dark matter as a manifestation of the GR modification [6]. The dark matter problem has long been a challenging issue for the theoretical physicists. On the experimental front, concerted efforts are being made to identify dark matter particles with masses of the order of hundreds of GeV scale. But till date, no such dark matter particles found from observations and experiments [4].

As per the observations, the Universe is mostly flat and isotropic and can be well explained by the standard ΛCDM model. However, certain observational data gathered in the last decade suggest a possible departure from the global isotropy. The high resolution cosmic microwave background (CMB) radiation data from Wilkinson Microwave Anisotropy Probe (WMAP) showing some large angle anomalies [7,8,9,10], a slight redshift of the primordial power spectrum of curvature perturbation from exact scale invariance as provided by the Planck data [11,12], observation of cosmic anisotropy due to unidirectional anisotropy of cosmic ray flow along the Galactic arms [13] seem to imply a violation of statistical isotropy. Other anomalies such as the lack of correlations on large angular scales, the hemi-spherical power asymmetry and the quadrupole-octupole alignment suggest a non-trivial topology of the large scale geometry of the Universe with an asymmetric expansion. Searches for large scale anisotropies are conventionally made by looking for non-uniformities in the distribution of events in right ascension [14,15].

Recently, from a maximum-likelihood analysis of the Joint Light Curve analysis catalogue of type Ia supernovae Colin et al. [16] found that, the deceleration parameter has a bigger dipole aligned with the cosmic microwave background dipole which rejects the statistical isotropy at 3.9σ statistical significance level. These observations obviously hint towards the scale invariance of the primordial perturbations and the possible presence of some anisotropic energy source in the universe with anisotropic pressure. In recent times, there have been some anisotropic models proposed to address the issue of the smallness in the angular power spectrum and departure from the global statistical isotropy [17,18,19,20] which bear a similarity to the Bianchi morphology [21,22,23].

In the present work, we have considered an anisotropic Universe where the dynamics is governed through dark energy. The dark energy pressure is assumed to be different along different spatial directions. This assumption stems from the fact of the anisotropy present in cosmic acceleration and CMB temperature anisotropy. Also, the possibility of primordial magnetic field may provide some sort of anisotropy to the model. The dynamical evolution of the pressure anisotropies have been studied in recent times by considering different space times and models [24, 25,26,27,28,29,30]. Therefore, our interest in the present work is to investigate the dynamical behaviour of the pressure anisotropies in an anisotropic Locally Rotationally Symmetric Bianchi I (LRSBI) metric and to correlate their dynamics to the evolutionary aspect of the deceleration parameter.

The paper is organized as follows: In Section 2, the basic formalism for anisotropic dark energy model with anisotropic pressures along different spatial

directions have been discussed for an anisotropic and spatially homogeneous LRSBI metric in the framework of General Relativity. The explicit expressions of the directional pressure anisotropies have been derived in terms of the Hubble parameter and deceleration parameter. In Section 3, we have considered some accelerating models and discussed the time evolution aspect of the pressure anisotropies. At the end, the summary and conclusions of the work are presented in Section 4.

2 Basic formalism

We consider an anisotropic dark energy model with anisotropic pressures along different spatial directions in the field equations in General Relativity, $G_{ij} \equiv R_{ij} - \frac{1}{2}Rg_{ij} = -T_{ij}$, where the energy momentum tensor for dark energy is assumed as

$$\begin{aligned} T_{ij} &= diag[\rho, -p_x, -p_y, -p_z] \\ &= diag[1, -\omega_x, -\omega_y, -\omega_z]\rho \\ &= diag[1, -(\omega+\delta), -(\omega+\gamma), -(\omega+\gamma)]\rho. \end{aligned} \tag{1}$$

The skewness parameters δ, γ are the respective deviations along $x-$ and $y-$ axes from the equation of state (EoS) parameter ω. We assume same pressure anisotropy along $y-$ and $z-$ axes. We allow these skewness parameters to evolve with the cosmic dynamics. ρ is the energy density and the pressure $p = \omega\rho$. Here we have used the gravitational units ($8\pi G = c = 1$). The line element for LRSBI space-time is considered in the form

$$ds^2 = -dt^2 + A^2dx^2 + B^2(dy^2 + dz^2), \tag{2}$$

where the directional scale factors $A = A(t)$ and $B = B(t)$ are functions of cosmic time only. Einstein field equations for the metric (2) are

$$\frac{2\dot{A}\dot{B}}{AB} + \left(\frac{\dot{B}}{B}\right)^2 = \rho, \tag{3}$$

$$\frac{2\ddot{B}}{B} + \left(\frac{\dot{B}}{B}\right)^2 = -(\omega+\delta)\rho, \tag{4}$$

$$\frac{\ddot{A}}{A} + \frac{\ddot{B}}{B} + \frac{\dot{A}\dot{B}}{AB} = -(\omega+\gamma)\rho. \tag{5}$$

An overhead dot on a field variable denotes differentiation with respect to time t. The energy conservation for the anisotropic fluid, $T^{ij}_{;j} = 0$, yields

$$\dot{\rho} + 3\rho(\omega+1)H + \rho(\delta H_x + 2\gamma H_y) = 0, \tag{6}$$

where the directional Hubble rates are defined as $H_x = \frac{\dot{A}}{A}$ and $H_y = \frac{\dot{B}}{B}$ and the mean Hubble rate is $H = \frac{1}{3}(H_x + 2H_y)$.

The above Eq. (6) can be split into two parts: the first one corresponds to the conservation of matter field with equal pressure along all the directions i.e. the deviation free part of (6) and the second one corresponds to that involving the deviations of EOS parameter:

$$\dot{\rho} + 3\rho(\omega+1)H = 0, \tag{7}$$

and

$$\rho(\delta H_x + 2\gamma H_y) = 0. \tag{8}$$

It is now certain that, the behaviour of the energy density ρ is controlled by the deviation free part of EOS parameter whereas the anisotropic pressures along different spatial directions can be obtained from the second part of the conservation equation. From Eq. (7), we obtain the energy density for a constant EOS parameter ω as $\rho = \rho_0 \mathcal{R}^{-3(\omega+1)}$, where ρ_0 is the value of energy density at the present epoch and $\mathcal{R}$ is the scale factor of the universe.

The scalar expansion θ and shear scalar σ^2 in the model are expressed as

$$\theta = (H_x + 2H_y)\,, \tag{9}$$

$$\sigma^2 = \frac{1}{2}\sigma_{ij}\sigma^{ij} = \frac{1}{2}\left(\Sigma H_i^2 - \frac{1}{3}\theta^2\right), \tag{10}$$

where $H_i; i = 1, 2, 3$ are the respective directional Hubble rates along $x-$, $y-$ and $z-$ axes. Also, $\sigma_{ij} = \frac{1}{2}(u_{i;k}h_j^k + u_{j;k}h_i^k - \frac{1}{3}\theta h_{ij})$ and $h_{ij} = g_{ij} - u_i u_j$ is the projection tensor. $u_i = \delta_i^0$ is the four velocity vector in the comoving coordinates. The shear scalar is usually considered to be proportional to the scalar expansion for spatially homogeneous metrics which leads to an anisotropic relationship among the directional scale factors A and B as $B = A^k$ [31,24]. Here k is a positive constant and represents the anisotropy in the model. The anisotropic relation can also be expressed as $H_y = kH_x$. Then the mean Hubble parameter becomes

$$H = \epsilon H_x, \tag{11}$$

where $\epsilon = \frac{3}{2k+1}$. The new parameter ϵ is a positive constant. Also it takes care of the anisotropic nature of the model. If ϵ is 1 than the model is isotropic and in all other case the model retains the anisotropic behaviour. One can note that, for $k = 1$, we have $\epsilon = 1$.

From Eq. (8) we obtain

$$\delta = -\left(\frac{3-\epsilon}{\epsilon}\right)\gamma. \tag{12}$$

From Eqs. (4), (5) and (12), we get the expressions for the pressure anisotropies along different directions as

$$\delta = \frac{(1-\epsilon)(3-\epsilon)}{2}\frac{F(H)}{\rho}, \tag{13}$$

$$\gamma = \frac{\epsilon(\epsilon-1)}{2}\frac{F(H)}{\rho}. \tag{14}$$

where $F(H) = \left(\dot{H} + 3H^2\right)$.

In GR, this functional $F(H)$ has a great role in ascertaining accelerating models [32]. If the functional $F(H)$ vanishes then accelerating models can not be achieved for LRSBI metric. This fact has already been shown in some earlier works [32,25,33]. However, in presence of some anisotropic sources such as the anisotropic dark energy components along different directions, we may obtain

a non vanishing functional $F(H)$ and therefore accelerating models can be well constructed [25,33].

The dynamical behaviour of the pressure anisotropies δ and γ is decided by the behaviour of the factor $\frac{F(H)}{\rho}$. This requires the behaviour of the energy density. The limiting value of the anisotropic parameter ϵ can be obtained from an analysis of the energy density. The expression for the energy density can be obtained from Eq. (3) as

$$\rho = \frac{3}{4}(3-\epsilon)(\epsilon+1)H^2. \tag{15}$$

The energy density of the universe should be positive throughout the cosmic evolution. In this sense, we have from Eq. (15), $\rho > 0$ for $\epsilon < 3$. Since $\epsilon = \frac{3}{2k+1}$, the limiting value k assumes is $k > 1$.

The factor $\frac{F(H)}{\rho}$ is evaluated as

$$\frac{F(H)}{\rho} = \frac{4}{3(3-\epsilon)(\epsilon+1)}(2-q), \tag{16}$$

where $q = -1 - \frac{\dot{H}}{H^2}$ is the deceleration parameter.

In terms of the deceleration parameter, the pressure anisotropies may be expressed as

$$\delta = \frac{2}{3}\left(\frac{1-\epsilon}{1+\epsilon}\right)(2-q), \tag{17}$$

$$\gamma = \frac{2}{3}\frac{\epsilon(\epsilon-1)}{(3-\epsilon)(\epsilon+1)}(2-q). \tag{18}$$

The above equations clearly indicate that, in an LRSBI dark energy dominated universe, the pressure anisotropies along different spatial directions depend on the evolutionary aspect of the deceleration parameter. If q is evolving with time, then the pressure anisotropies will evolve otherwise we get constant pressure anisotropies. In order to get an idea of the total anisotropies, we may take a sum

$$\delta + \gamma = \frac{2}{3}\frac{(1-\epsilon)(3-2\epsilon)}{(3-\epsilon)(\epsilon+1)}(2-q). \tag{19}$$

3 Some accelerating models

In this section, we wish to investigate some accelerating models by considering some well known forms of the Hubble parameter. Our interest is to study the evolutionary behaviour of the anisotropic dark energy pressure along different spatial directions. The commonly known accelerating models as available in literature are the de Sitter model (H=constant), the power law expansion of the scale factor and the hybrid scale factor.

3.1 de Sitter model (H=constant)

As a first case, we consider the de Sitter model where the universe expands exponentially with time. The de Sitter expansion model is represented through a constant Hubble parameter

$$H = H_0, \tag{20}$$

where H_0 is a constant and is equal to the Hubble parameter as measured in the present epoch. Obviously for this model, the deceleration parameter becomes $q = -1 - \frac{\dot{H}}{H^2} = -1$.

We can obtain the expression for the functional $F(H)$ for the de Sitter model as

$$F(H) = 3H_0^2. \tag{21}$$

The energy density ρ may be obtained as

$$\rho = \frac{3}{4}(3-\epsilon)(\epsilon+1){H_0}^2. \tag{22}$$

Since the Hubble parameter is a constant quantity, the dark energy density for this model becomes a constant quantity. It should be recalled here that we have considered only dark energy as the contributing factor to the matter field. Along with the dark energy, we have considered some unknown sources for anisotropic dark energy pressure along different spatial directions.

The pressure anisotropies along different spatial directions such as δ and γ are obtained as

$$\delta = \frac{3}{2\rho}(1-\epsilon)(3-\epsilon)H_0^2, \tag{23}$$

$$\gamma = \frac{3}{2\rho}\epsilon(\epsilon-1)H_0^2. \tag{24}$$

Since the energy density can be expressed in terms the Hubble parameter, we may write the pressure anisotropies as

$$\delta = 2\left(\frac{1-\epsilon}{1+\epsilon}\right), \tag{25}$$

$$\gamma = -2\left(\frac{\epsilon}{3-\epsilon}\right)\left(\frac{1-\epsilon}{1+\epsilon}\right). \tag{26}$$

It is interesting to note that, the pressure anisotropies come out to be constant quantities for this model. In other sense, if we enforce a constant anisotropic dark energy source which results in a non evolving dark energy density leads to constant finite pressure anisotropies along different spatial directions. Also, for such a situation, the pressure anisotropy is maintained throughout the cosmic evolution for the de Sitter model. In order to get a quantitative view of the pressure anisotropies, we may consider some representative values for the anisotropic parameter ϵ namely $\epsilon = 0.9$ and 0.95. For these representative values of ϵ we get δ respectively as 0.105 and 0.051. Similarly, the pressure anisotropy along yz plane is obtained to be -0.045 and -0.024 respectively. With an increase in the value of ϵ, the pressure anisotropy along the x-axis decreases but the pressure anisotropy along the yz plane increases. Another fact is that, while δ becomes a positive quantity, we obtain γ as a negative quantity.

The sum of the pressure anisotropies for the present model become

$$\delta + \gamma = 2\frac{(1-\epsilon)\,(3-2\epsilon)}{(3-\epsilon)\,(1+\epsilon)}. \tag{27}$$

For the representative values of the anisotropic parameter ϵ, we have sum of the pressure anisotropies as 0.06 and 0.027. With an increasing value of ϵ towards

1, it may be found that, the sum of the pressure anisotropies vanishes.

3.2 Power law expansion of the scale factor

Here we consider a power law expansion model of the universe where the scale factor of the model increases as $\mathcal{R} = t^m$, m being a positive constant. Power law expansion models are very popular in addressing many issues in cosmology. The Hubble parameter for this model can be expressed as

$$H = \frac{m}{t}. \tag{28}$$

The deceleration parameter for power law expansion model becomes

$$q = -1 + \frac{1}{m}. \tag{29}$$

An accelerating model is characterized by a negative deceleration parameter. This fact restricts the parameter m in the range $m > 1$.

For the power law expansion model, the energy density may be calculated as

$$\rho = \frac{3m^2}{4}\frac{(3-\epsilon)(\epsilon+1)}{t^2}, \tag{30}$$

which is obviously positive for a choice of $\epsilon < 3$ and $m > 1$.

The functional $F(H)$ for the present power law expansion model becomes

$$F(H) = \frac{m}{t^2}(3m-1), \tag{31}$$

and consequently, the directional pressure anisotropies γ and δ would be

$$\delta = \frac{2}{3}\left(\frac{1-\epsilon}{1+\epsilon}\right)\left(3-\frac{1}{m}\right), \tag{32}$$

$$\gamma = \frac{2}{3}\frac{\epsilon(\epsilon-1)}{(3-\epsilon)(\epsilon+1)}\left(3-\frac{1}{m}\right). \tag{33}$$

In this case also, we get constant pressure anisotropies along different spatial directions. The sum of the pressure anisotropies becomes

$$\delta + \gamma = \frac{2}{3}\frac{(1-\epsilon)(3-2\epsilon)}{(3-\epsilon)(\epsilon+1)}\left(3-\frac{1}{m}\right). \tag{34}$$

In order to get a quantitative view of the pressure anisotropies, we choose some representative values of the anisotropic parameter ϵ and the model parameter m. As before, we consider $\epsilon = 0.9$ and 0.95. For m, we have a restriction on it such as $m > 1$. This is required to get an accelerating model. In view of this, we chose $m = 1.1$. For $\epsilon = 0.9$, we get $\delta = 0.073$ and $\gamma = -0.031$. For $\epsilon = 0.95$, we obtain $\delta = 0.036$ and $\gamma = -0.017$. With an increase in ϵ, while there is an increase in γ, there is a decrease in the value of δ.

3.3 Hybrid scale factor

The late time cosmic speed up issue has triggered many novel ideas and concept. Within the purview of the GR, the exotic dark energy is an obvious choice to

explain the late time cosmic acceleration. Another important issue concerning the late time cosmic acceleration phenomena is that whether the Universe has undergone a transition from an early deceleration to late time acceleration. If so, then what is the time frame within which such a transition has occurred? Usually, the acceleration or deceleration of the cosmic expansion is assessed through the deceleration parameter q. If $q < 0$, the model is assumed to be accelerating on the other hand if $q > 0$ the model is considered to be decelerating. Basing upon the analysis of the deceleration parameter, we may define a transition redshift z_t at which the deceleration parameter becomes zero i.e. $q = 0$. It is believed that, if at all there has occurred a late time cosmic acceleration, then the transition redshift z_t may be regarded as a fundamental constant parameter! In many studies, this quantity has been constrained in order of unity, i.e. $z_t \sim 1$. One interesting similarity of the power law expansion model or the de Sitter expansion model is that, both may provide accelerating models but with a non-evolving deceleration parameter. In the context of a transitioning universe, it is required that the deceleration parameter should be evolving in nature with a signature flipping behaviour. Such a scenario may be simulated through the concept of a hybrid scale factor (HSF) defined through a Hubble parameter [33]

$$H = \alpha + \frac{\beta}{t}, \tag{35}$$

where α and β are positive constants. The deceleration parameter for the HSF model may be expressed as $q = -1 + \frac{\beta}{(\alpha t+\beta)^2}$. Considering suitable parameters of the HSF model, it is possible to model transitioning universe with early deceleration and late time acceleration.

For the HSF model, we obtain the energy density as

$$\rho = \frac{3}{4}(3-\epsilon)(\epsilon+1)\left(\alpha + \frac{\beta}{t}\right)^2, \tag{36}$$

and the functional $F(H)$ as

$$F(H) = \frac{\beta(3\beta-1)}{t^2} + \frac{6\alpha\beta}{t} + 3\alpha^2. \tag{37}$$

The expressions of the directional pressure anisotropies γ and δ become

$$\delta = \frac{2}{3}\left(\frac{1-\epsilon}{1+\epsilon}\right)\left(3 - \frac{\beta}{(\alpha t+\beta)^2}\right), \tag{38}$$

$$\gamma = \frac{2}{3}\frac{\epsilon(\epsilon-1)}{(3-\epsilon)(\epsilon+1)}\left(3 - \frac{\beta}{(\alpha t+\beta)^2}\right). \tag{39}$$

It is interesting to note here that, the pressure anisotropies in this HSF model are evolving with time. This fact has come from the time evolution of the deceleration parameter. In order to understand the time evolution of the pressure anisotropies in HSF model, we have considered some recently constructed HSF models with parametric value as given in the Table 1 [34, 35]. These models have been constructed from the observational $H(z)$ data.

In Fig. 1(a) and (b), the time evolution of the parameters representing the pressure anisotropies along different spatial directions are shown for the four models

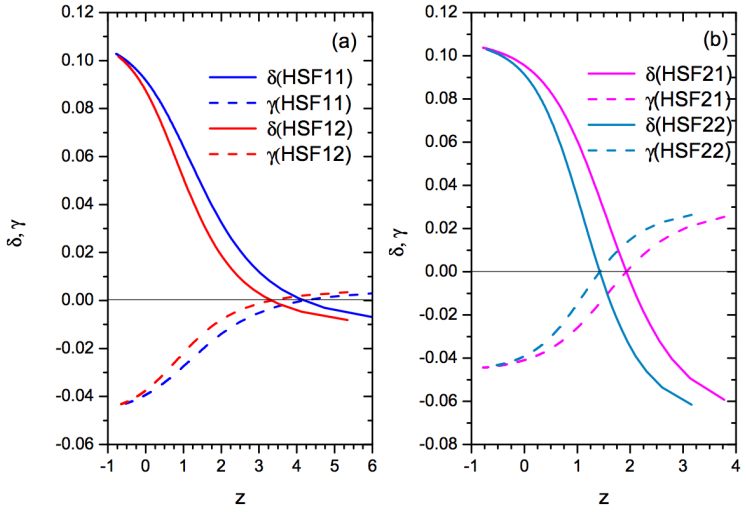

Fig. 1 (a) The pressure anisotropies δ and γ for the hybrid scale factor models HSF11 and HSF12, (b) same as (a) for the models HSF21 and HSF22. Here we have considered the anisotropic parameter as $\epsilon = 0.9$.

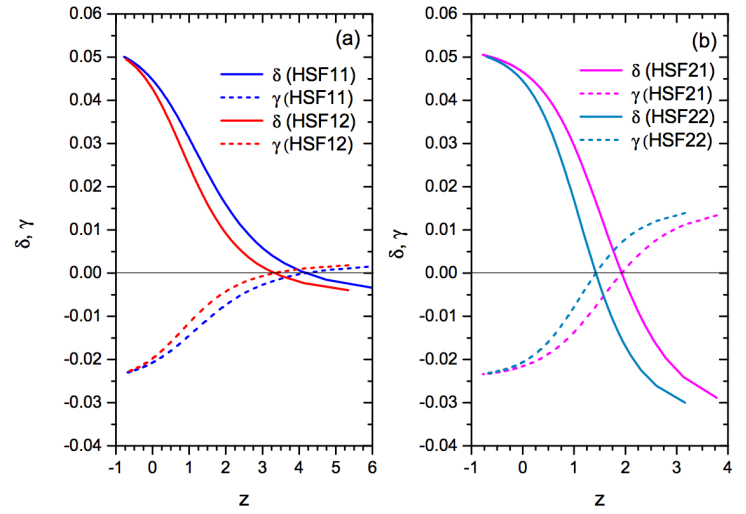

Fig. 2 (a) The pressure anisotropies δ and γ for the hybrid scale factor models HSF11 and HSF12, (b) same as (a) for the models HSF21 and HSF22. Here we have considered the anisotropic parameter as $\epsilon = 0.95$.

Table 1 Model parameters of the hybrid scale factor [34,35].

Models	β	α	z_t	z_r
HSF11	0.3	0.585	0.8	4.05
HSF21	0.2	0.65	0.8	1.925
HSF12	0.3	0.47	0.5	3.517
HSF22	0.2	0.51	0.5	1.448

where we have considered $\epsilon = 0.9$. The same has been repeated in Fig. 2(a) and (b) for $\epsilon = 0.95$. The upper solid curves represent the evolution of δ and the lower dashed curves represent the evolutionary aspects of γ. We have considered the figures upto a reasonable value of redshift around $z = 6$. Within these time frame, we observe that, while δ increases with cosmic expansion, γ decreases. There occurs a signature reversal in the behaviour of the pressure anisotropies δ and γ. We denote the redshift at which the signature flipping in δ and γ occurs as z_r. It is found that, z_r depends on the HSF model chosen but is independent of the choice of the anisotropic parameter ϵ. The reversal redshift as obtained for the four HSF models are $z_r = 4.05, 1.925, 3.517$ and 1.448 corresponding to the HSF models HSF11, HSF21, HSF12 and HSF22. One should note that, the behavioural reversal redshift z_r is quite different than the transition redshift z_t, even though both are of the order of unity.

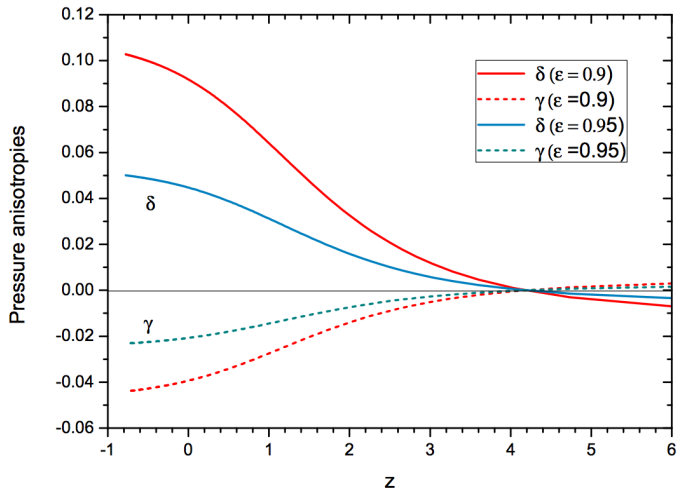

Fig. 3 The effect of ϵ on δ and γ is shown for the model HSF11.

In Fig. 3, we show the effect of the anisotropic parameter ϵ on any given HSF model within the formalism discussed in the present work. Here we have considered only the HSF11 model. It is obvious from the figure that, with an increase in

the value of ϵ, the magnitudes of the pressure anisotropies decrease substantially. Also, a change in the value of ϵ does not affect the behavioural reversal redshift z_r. Similar conclusion may be inferred for all other HSF models.

4 Summary and conclusion

In the present work, we have discussed some accelerating models supported by some anisotropic dark energy. We have assumed different pressure along different spatial directions in the back drop of an anisotropic LRSBI metric. The departure of the directional pressures from the isotropic pressure are assumed to be characterized by some directional pressure anisotropies. Assuming some specific forms of accelerating Hubble parameters, we have derived the expressions of the directional pressure anisotropies and expressed them in terms of the deceleration parameter. It is shown that, the evolutionary aspects of the pressure anisotropies directly depend on the evolutionary behaviour of the deceleration parameter. Three different forms of the Hubble parameter are considered namely, the de Sitter scenario, the power law expansion and the hybrid function. Out of these three forms, the first two provide a constant deceleration parameter whereas the third function provides a signature flipping behaviour of the deceleration parameter with early epoch positive values and late epoch negative values. Since the evolutionary aspects of the pressure anisotropies are associated with the time evolution of the deceleration parameter, in the first two cases, we obtain constant pressure anisotropies which are maintained through out the cosmic evolution.

HSF is required to simulate a signature flipping deceleration parameter that provides a realistic picture of the transitioning Universe from early deceleration to late time acceleration. We have considered four different models of the HSF to investigate the evolutionary aspects of the pressure anisotropies along different directions. It is certain that, since the deceleration parameter for HSF models evolve with time, the pressure anisotropies also evolve with time. While the pressure anisotropy along the x-axis increases with cosmic evolution, the pressure anisotropy along the symmetry plane decreases with time. An interesting behaviour is seen in the evolutionary aspects of the pressure anisotropies. Both of them reverse their signatures at certain behavioural reversal redshift which depends on the model chosen. We have also examined the effect of the anisotropic parameter on the evolution of the pressure anisotropies and found that, with an increase in the value of the anisotropic parameter, the magnitudes of the pressure anisotropies decrease substantially.

Acknowledgement

The present work is an outcome of some discussions held during a workshop on General Relativity, Gravitation and Cosmology organized by the Physics Forum, Indira Gandhi Institute of Technology, Sarang, India. SKT, BM and SR acknowledge the support of IUCAA, Pune, India through the visiting associateship program.

References

1. A.G. Riess et al., *Astron. J.* **116** (1998) 1009.

2. S. Perlmutter et al., *Astrophys. J.* **517** (1999) 565.
3. N. Aghanim et al. [Planck Collaboration], *Astron. Astrophys.* **641** (2020) A6.
4. G. Bertone, D. Hooper and J. Silk, *Phys. Rept.* **405** (2005) 279.
5. D. Hooper and S. Profumo, *Phys. Rept.* **453** (2007) 29.
6. S. Capozziello and M. De Laurentis, *Ann. Phys.* **524** (2012) 545.
7. G. Hinshaw et al., *Astrophys J. Suppl. Ser.* **170** (2007) 288.
8. G. Hinshaw et al., *Astrophys J. Suppl. Ser.* **180** (2009) 225.
9. A. de Oliviera-Costa, M. Tegmark, M. Zaldarriaga and A. Hamilton, *Phys. Rev. D* **69** (2004) 063516.
10. M. Watanabe, S. Kanno and J. Soda, *Phys. Rev. Lett.* **102** (2009) 191302.
11. P.A.R. Ade et al. (Planck Collaboration), *Astron. Astrophys.* **571** (2014) A1.
12. P.A.R. Ade et al. (Planck Collaboration), *Astron. Astrophys.* **571** (2014) A16.
13. S.M. Moghaddam and M. Bahmanabadi, *Phys. Rev. D* **97** (2018) 062001.
14. IceCube Collaboration, *Astrophys. J.* **866** (2016) 220.
15. KASCADE Collaboration, *Nucl. Part. Phys. Proc.* **279** (2016) 56.
16. J. Colin, R. Mohayaee, M. Rameez and S. Sarkar, *Astron. Astrophys.* **631** (2019) L13.
17. L. Campanelli, P. Cea and L. Tedesco, *Phys. Rev. Lett.* **97** (2006) 131302.
18. L. Campanelli, P. Cea and L. Tedesco, *Phys. Rev. D* **76** (2007) 063007.
19. L. Campanelli, *Phys. Rev. D* **80**(2009) 063006.
20. A. Gruppo, *Phys. Rev. D* **76** (2007) 083010.
21. J. Jaffe et al., *Astrophys J.* **629** (2005) L1.
22. J. Jaffe et al., *Astrophys J.* **643** (2006) 616.
23. J. Jaffe et al., *Astron. Astrophys.* **460** (2006) 393.
24. B. Mishra, P.K. Sahoo and S.K. Tripathy, *Astrophys. Space Sci.* **356** (2015) 261.
25. S.K. Tripathy, B. Mishra and P.K. Sahoo, *Eur. Phys. J. Plus* **132** (2017) 388.
26. B. Mishra, S.K. Tripathy and P.P. Ray, *Astrophys. Space Sci.* **363** (2018) 86.
27. P.P. Ray, B. Mishra and S.K. Tripathy, *Int. J. Mod. Phys. D* **28** (2019) 1950093.
28. B. Mishra, P.P. Ray, S.K. Tripathy and K. Bamba, *Mod. Phys. Lett. A* **34** (2019) 1950217.
29. B. Mishra, P.P. Ray and R. Myrzakulov, *Eur. Phys. J. C* **79** (2019) 34.
30. S.K. Tripathy, B. Mishra, M. Khlopov and S. Ray, *Int. J. Mod. Phys. D* (2021) DOI:10.1142/S0218271821400058.
31. S.K. Tripathy, D. Behera and T.R. Routray, *Astrophys. Space Sci.* **325** (2010) 93.
32. S.K. Tripathy, *Astrophys. Space Sci.* **350** (2014) 367.
33. B. Mishra and S.K. Tripathy, *Mod. Phys. Lett. A* **30** (2015) 1550175.
34. S.K. Tripathy, S.K. Pradhan, P. Parida, D. Behera, R.K. Khuntia and B. Mishra, *Phys. Scr.* **95** (2020) 115001.
35. S.K. Tripathy, S.K. Pradhan, Z. Naik, D. Behera and B. Mishra, *Phys. Dark. Univ.* **30** (2020) 100722.

Scientific Voyage
Vol. 2, No. 3,
Page 21-28 (2021)

SCIENTIFIC VOYAGE
ISSN: 2395-5546

GCECT
Publication
July - Sept.

In-situ remediation of mine soils with biochar and evaluation of its effectiveness

Soham Ray*

Department of Genetics, Institute of Genetic Engineering, 30 Thakurhat Road, Badu, Madhyamgram, Kolkata 700128, W.B., India

Abstract: In this report we briefly present in-situ remediation of mine soils with biochar and and evaluation of its effectiveness with *Acacia auriculiformis* plant and *Azospirillum* bacteria.

Keywords: bioremediation; mine soil; biochar; acacia auriculiformis; azospirillum

1 Introduction

The term ‘phyto’ means plant and 'remediation' means reversing of environmental damage. Phytoremediation is a generic group of technologies that use specific plants for bioremediating soils, sludges, sediments and water contaminated with organic and inorganic contaminants. It involves growing plants in a contaminated matrix (soil, water or sediments) for a required growth period, to remove or facilitate immobilization or degradation of the pollutants [1,2].Among various techniques used to remediate mine soil one effective strategy is by amendment of the mine soil with biochar. The word ‘biochar’ is a combination of ‘bio’ as in ‘biomass’and ‘char’ as in ‘charcoal’. It is a high-carbon, fine-grained residue that today is produced through pyrolysis processes like direct thermal decomposition of biomass in the absence of oxygen (preventing combustion), which produces a mixture of solids (the proper biochar), liquid (bio-oil) and gas (syngas) products [3,4].

The main purpose or motivation of the study is as follows. Mine soils in different locations around the world pose a serious problem of environmental pollution with the release and accumulationof heavy metalsand metalloids. It also leaches into neighbouring areas causing severe toxicity to local and surrounding plants, cattle, aquatic and human populations. Thus, there is need to mitigate those problems caused near mine areas as part of post mining procedures [2]. Biochar is effective at retaining both water as well as water-soluble nutrients and reduce leaching due to its hygroscopic and porous structure. It is a suitable habitat for many beneficial soil micro-organisms and it has also shown to increase soil fertility and improve disease resistance in soils [4,5].

2 Objectives

(i) To investigate the potential of biochar to remediate sample soils from Dhanbad coal mines, India in a pot experiment with *Acacia auriculiformis* plant and *Azospirillum* bacteria.

(ii) To check if there are any toxic or hazardous effects of using biochar on plants through Allium genotoxicity test.

* **Present address:** Department of Bio-diversity, Tomsk State University, Lenin Ave, 36 Tomsk, Tomsk Oblast 634050, Russia

3 Literature survey

3.1 Bioremediation of soils with the help of biochar

Qin et al. [5] reported in their study that biochar has the potential to reduce toxicity of petroleum contaminated soils in China. It was found that the biochar made from rice straw could absorb petroleum metabolites. With the help of soil micro-cosmitit was found that biochar has the ability to degrade contaminants in soil. The degrading efficiency was significantly higher in soils amended with biochar than in soils without biochar. It was also shown that biochar did not result in negative impacts on the composition of soil microbial community.

3.2 *Acaciaauriculiformis* as a metal hyperaccumulating plant

Acacia auriculiformis is a fast growing tree in the family Fabaceae, originating from Australia and having densely matted root system which makes it suitable for stabilizing eroded land. It has been used for water and soil conservation and also to improve soil fertility in barren regions of South China. Its extraordinary drought tolerant and metal resistant capabilities along with high biomass production makes it an ideal plant species for phytoremediation [9].

3.3 Azospirillum as a plant growth promoter in biotic stress

Azospirillum is a Gram-negative, microaerophilic, non-fermentative and nitrogen-fixing bacterial genus from the family of Rhodospirillaceae. Azospirillum bacterium fixes the atmospheric nitrogen and makes it available to plants in non-symbiotic manner that can replace 50-90 % and of the nitrogen fertilizer required by plants and enhances the plant growth. Azospirillum is also a biofertilizer and can also promote plant growth by mechanisms of tolerance of abiotic and biotic stresses [6,7,8].

4 Materials and methods

4.1 Preparation of biochar

Eucalyptus tree bark was pyrolysed at pyrolysing chamber in Department of Environmental Science & Engineering, Indian Institute of Technology, Kharagpur. Two varieties were prepared: (i) Pyrolysed at 400 °C for 45 minutes.(ii) Pyrolysed at 600 °C for 45 minutes. Biochar was then crushed to powder form with ball mill in Department of Mining Engineering, Indian Institute of Technology, Kharagpur.

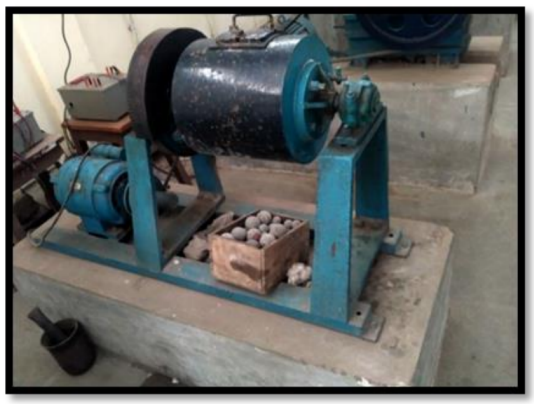

Figs. 1 & 2: Pyrolysis chamber and Ball mill

4.2 Composition of soil samples

Each pot test sample carried 2kg of mine soil from coal mines of Dhanbad in the state of Chattisgarh, India. Biochar in crushed powder form was mixed uniformly with those pot test samples. Six controls were also used in the study. Two of which contained 10^8 CFU of Azospirillum in 2 kg of mine soil. Two of the positive controls C3 and C4 contained mine soils only. Other two werenegative controls C1-S and C2-S containing Azospirillum only. The remaining C - F contained fertilizer with mine soil.

Sample ID	**Biochar(gm)**	**Sample ID**	**Biochar (gm)**	**Sample ID**	**Ingredients**
0.5B1C	10	0.5B1C- NP	10	C1 - S	*Azospirillum*
1B1C	20	1B1C - NP	20	C2 – S	*Azospirillum*
2B1C	40	2B1C - NP	40	C3	Mine soil
5B1C	100	5B1C -NP	100	C4	Mine soil
10B1C	200	10B1C - NP	200	C – F	Fertilizer
0.5B2C	10	0.5B2C- NP	10		
1B2C	20	1B2C - NP	20		
2B2C	40	2B2C - NP	40		
5B2C	100	5B2C -NP	100		
10B2C	200	10B2C - NP	200		

Table 1: Composition of soil samples

Fig. 3: Soil samples with different biochar concentrations

4.3 Study design and greenhouse

A pot study was designedin which several pots for different concentrations of mine soil was amended with test material biochar. The pots were kept at a small greenhouse near the Department of Mining Engineering, Indian Institute of Technology, Kharagpur, India.

Fig. 4: Pots inside greenhouse

4.4 Estimation of plant leaf chlorophyll content

For the estimation of chlorophyll A, chlorophyll B and total carotenoid content in *Acacia auriculiformis* leaves, the standard procedure as performed by Dere et al. [10] was followed.

(i) 5 gm of leaf samples were crushed separately in 95% diethyl ether (50 ml for each gram).
(ii) Samples were homogenized & centrifuged at 2500 rpm for ten minutes & the supernatant was separated.
(iii) Absorbance was read on spectrophotometer by the formula given in Table 2.

Table 1. The formulas that used in the calculation of chlorophyll a, chlorophyll b and total caroten levels

Diethyl ether	$C_a = 10.05\ A_{662} - 0.766\ A_{644}$ $C_b = 16.37\ A_{644} - 3.140\ A_{662}$ $C_{x+c} = 1000\ A_{470} - 1.280\ C_a - 56.7\ C_b/230$
Methanol	$C_a = 15.65\ A_{666} - 7.340\ A_{653}$ $C_b = 27.05\ A_{653} - 11.21\ A_{666}$ $C_{x+c} = 1000\ A_{470} - 2.860\ C_a - 129.2\ C_b/245$
Acetone	$C_a = 11.75\ A_{662} - 2.350\ A_{645}$ $C_b = 18.61\ A_{645} - 3.960\ A_{662}$ $C_{x+c} = 1000\ A_{470} - 2.270\ C_a - 81.4\ C_b/227$

C_a = Chlorophyll a, C_b = Chlorophyll b, C_{x+c} = Total carotene

Table 2: Formulas for estimation of chlorophyll content

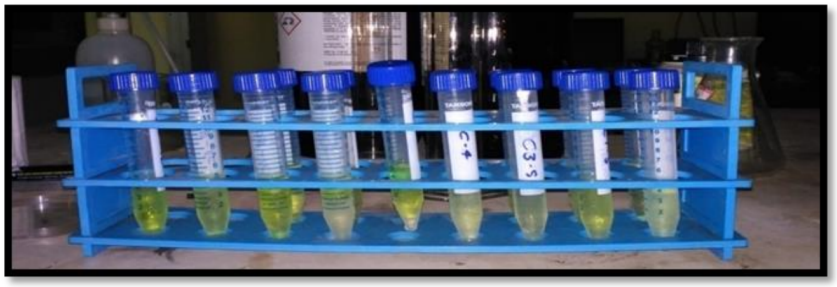

Fig. 5: Leaves homogenized in 95% Diethyl Ether

4.5 CFU count of Azospirillum bacteria

10^8 CFU/ml of Azospirillum was cultured in Azospirillium growth media in Department of Mining Engineering, Indian Institute of Technology, Kharagpur, India. In the test soil samples 1 ml of Azospirillum was taken in 50 ml of 0.85% saline distilled water and then mixed uniformly with 2 kg of test soil samples. Thus theoretically, there was 1 ml or 10^8 CFU of Azospirillum in those selected pot soils. Therefore, 1 gm of those soil should contain 50,000 CFU which can be taken as the comparable measure of Azospirillum at the starting point of the experiment. After 3 months those bacteria from pot soils were diluted upto 10^{-4} times and pour plated in selective Azospirillum medium for colony count.

5 Results and discussion

5.1 Plant shoot growth

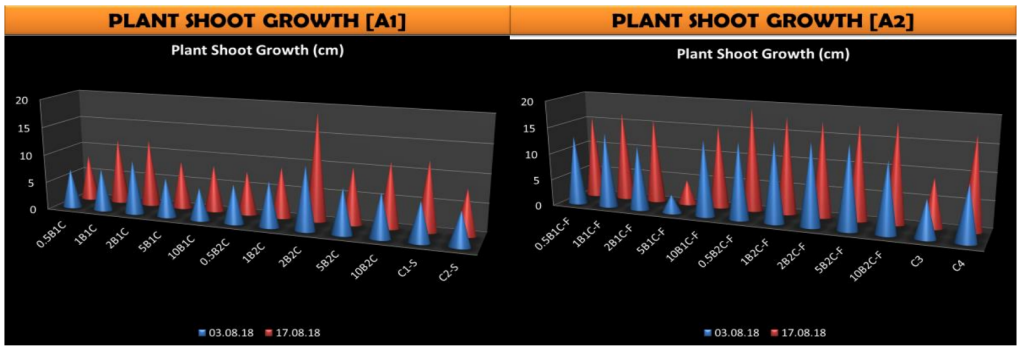

Tables 4&5: *Acacia* plant shoot growth from 03.08.2018 to 17.08.2018

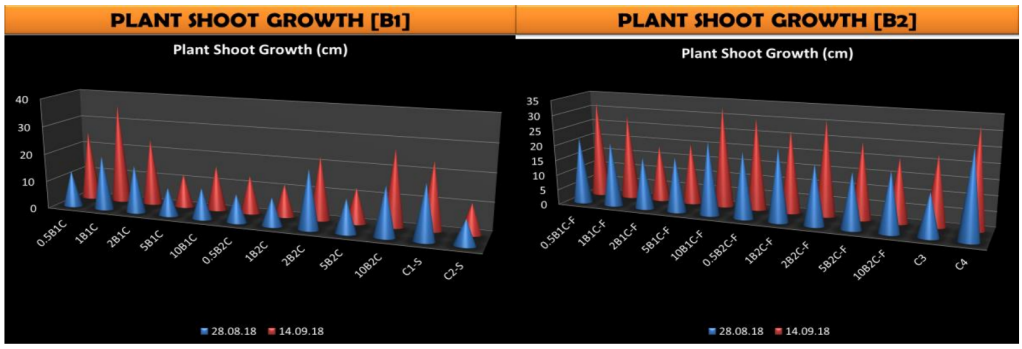

Tables 6&7: *Acacia* plant shoot growth from 28.08.2018 to 14.09.2018

From the above tables it can be seen that plant shoot growth is slightly higher in samples with both biochar and fertilizer inclusion when compared with controls and samples with only biochar amended soil.

5.2 Leaf chlorophyll content

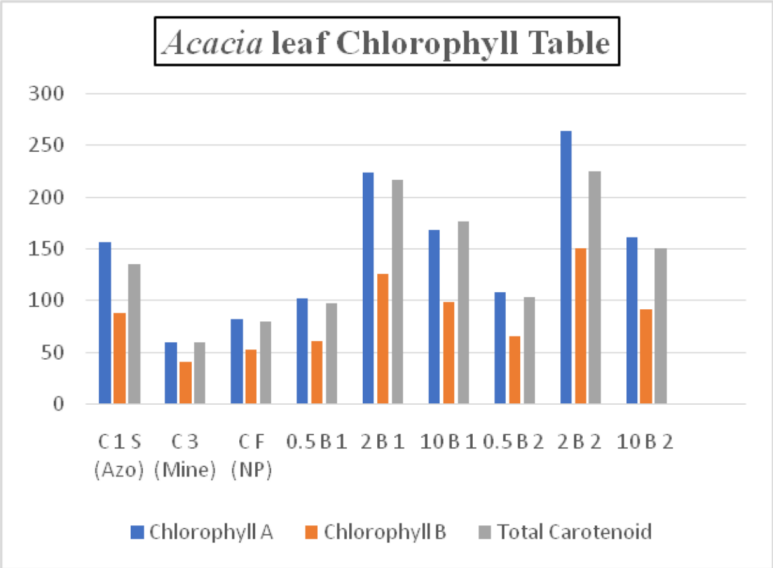

Table 8: *Acacia* leaf chlorophyll content

From the above table it can be seen that chlorophyll A, chlorophyll B and total carotenoid content was significantly higher in soil samples amended with biochar. The samples 2B1 and 2B2 which contained 40gm/kg biochar showed the most positive results.

5.3 Bacteria CFU count

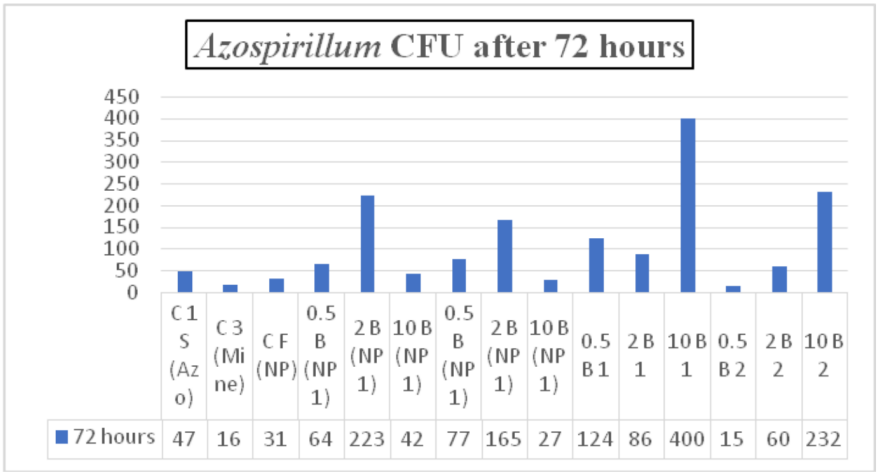

Table 9: *Azospirillum* CFU after 72 hours incubation

From the above table it can be seen that *Azospirillum* bacteria had higher viability rates in biochar amended soils. Here the soils amended only with biochar showed significantly higher bacteria viability rate than controls and fertilizer included biochar soils with 10B1 and 10B2 being the highest of them all.

Fig. 6: CFU count in petri plates

7 Conclusion

Medium dosage of biochar at 40 gm/kg of mine soil to be amended was found to possess the highest remediation potential among dosages of 10gm/kg, 20gm/kg, 40gm/kg, 100gm/kg and 200gm/kg of biochar in mine soils of Dhanbad coal dump region, state of Jharkhand, India. The remediation potential can be well proven altogether with similar patterns of data coming from plants and microbes which can be summed up as –

Acacia auriculiformis shoot growth data; *Acacia auriculiformis* leaf chlorophyll a, b and total carotenoid content; higher viability of *Azospirillum* colony forming units tested in biochar amended soil.

Acknowledgements:

The work presented here was performed as a part of the Summer Internship at Department of Mining, Indian Institute of Technology, Kharagpur, West Bengal, India and I express my gratitude to Professor (Dr.) Jayanta Bhattacharya for providing me with the facilities and permission for this work. I am thankful to Mr. Subhas Chandra for his scientific supervision and guidance in this work. I am also thankful to my father Dr. Saibal Ray for his constant inspiration for this investigation.

References

1. A. Mandal, T.J. Purakayastha, S. Ramana, S. Neenu, D. Bhaduri, K. Chakraborty, M.C. Manna and A.S. Rao, *Int. J. Bio-resource and Stress Manage.* **5** (2014) 553.
2. S.P. McGrath, F.J. Zhao and E. Lombi, *Plant Soil.* **232** (2001) 207.

3. University of Barcelona, "Reducing mineral fertilisers and agro-chemicals by recycling treated organic waste as compost and biochar products Framework Programme 7 (FP7)", *Social Impact Open Repository* (2011-2015).
4. B.M.D. Kanouo, S.E. Allaire and A.D. Munson, *Waste Biomass Valor*. **9** (2018) 899.
5. G. Qin, D. Gong and M.-Y. Fan, *Int. Biodeter. Biodegrad.* **85** (2013) 150.
6. O. Steenhoudt and J. Vanderleyden, *FEMS microbial. Rev.* **24** (2000) 487.
7. J. Fukami, P. Cerezini and M. Hungria, *AMB Express* **8** (2018) 73.
8. A. Karthikeyan and M.S. Prakash, *Forests, Trees and Livelihoods* **18** (2008) 183.
9. A.Z. Sofea, A. Zerkout, A.A.N. Azwady, G. Rusea and M. Muskhazli, *Ann. Res. Rev. Bio.* **18** (2017) 1.
10. S. Dere, T. Gunes and R. Sivaci, *Tr. J. Bot.* **22** (1998) 13.
11. A Grant. W.F. “Chromosome aberration assays in Allium - A report of the U.S. Environmental Protection Agency Gene-Tox Program”, Mutation Research, 99 (1982) 273-291 (Elsevier Biomedical Press).

Scientific Voyage
Vol. 2, No. 3,
Page 29-33 (2021)

SCIENTIFIC VOYAGE
ISSN: 2395-5546

GCECT
Publication
July - Sept.

The founder of the Quantum Mechanics Max Planck as Nobel Prize nominator – praxis of his nomination

Rajinder Singh[1] and Björn Martens [2]

Research Group - Physics Didactic and Science Communication, Institute of Physics, University of Oldenburg, Germany

Abstract: The German physicist Max Planck (1858-1947) was awarded the Physics Nobel Prize for the year 1918. From 1901 to 1937, he nominated various scientists for the Physics Nobel Prize. His nomination letter were acquired by us from the archive of the Royal Swedish Academy of Sciences, Stockholm. Result of their analysis is given in this short communication.

Keywords: Max Planck; Quantum Mechanics; Nobel Prize

1 Introduction

In literature we find M. Planck's life and science [1,2,3] and nomination for the Nobel Prize [4]. In our previous article, we discussed: (i) Scientific work for which Planck was nominated for the Nobel Prize, and (ii) Opinions of his nominators. (iii) Short biography [5].

However, in the published literature, Planck's role as a nominator has not been discussed. The present article intends to fill the gap.

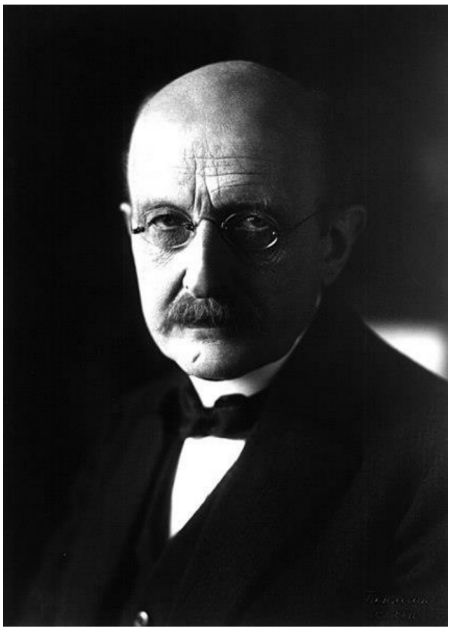

Fig. 1: Max Planck [*Credit: Wiki (Public domain)*]

[1] Email: rajinder.singh@uni-oldenburg.de

[2] Email: Bjoern.Martens@uni-oldenburg.de

2 Planck as Nominator

Year	Nominee/s	Nation	Candidate nominated for	NP awarded in
1901	W.C. Roentgen	GER	Radiation named after him [6]	1901
1902	H.A. Lorentz [7]	NDL	None [8]	1902
1902/1903/1904	J.W. Strutt (Lord Rayleigh)	GBR	Discovery of Argon gas [9]	1904
1905/1906	L. Boltzmann	AUT	Research in the field of kinetic theory of gases, and his book "Lectures on Gas Theory" [10]	-
1907/1908	E. Rutherford	CAN	Radioactivity [11]	1908 (CNP)
1911	W. Nernst	GER	Number of experimental and theoretical works, in particular his land mark investigation on the electromotive effectiveness of ions [12]	1920 (CNP)
1916	J. Stark	GER	Discovery of the Doppler-Effect in Canal Radiation [13]	1919
1919/1920/1921	A. Einstein	GER	General Theory of relativity [14]	1921
1922	N. Bohr	DNK	Spectroscopy and atomic model [15]	1922
1923/1924/1925/ 1926/1928/1929/ 1932/1933	F. Paschen & A. Sommerfeld	GER	Fine-structure of spectral lines (experiment & theory) [16]	- & -
1927	A.H. Compton [17]	USA	For the effect named after him [18]	1927
1930	W. Heisenberg	GER	Development of Quantum Mechanics [19]	1932
	E. Schroedinger	AUT	Development of Quantum Mechanics [20]	1933
1931	O. Stern	GER	Investigations on the atomic- and molecular radiation [21]	1943
1934	O. Stern	GER/ USA	Atomic/Molecular radiation; Proof of Maxwell's law of velocity distribution [22]	
1935	W. Pauli	CHE	Discovery named after him ("Pauli exclusion principle") [23]	1945
1936	C.D. Anderson [24]	USA	Discovery of positrons [25]	1936
1937	E. Fermi	ITA	His investigations in the field of atomic physics; particularly artificial radioactivity [26]	1938
1947	L. Meitner	SEW	No statement by Planck [27]	-

Table 1: Data collected from Planck's correspondence, and literature. Scientists nominated for the Physics Nobel Prize by M. Planck. Abbreviations: AUT – Austria, CAN – Canada, CHE – Switzerland, GER – Germany, DK – Denmark, ITA – Italy, SEW–Sweden, GBR – United Kingdom, USA – United States of America. CNP – Chemistry Nobel Prize.

From the foregoing we see that in the first decade of the twentieth century, Planck was very successful nominator. He nominated five persons. Out of them four received the Nobel Prize in the year of nomination. Also, we see that all of his nominees were from different countries.

In the second decade, he nominated three German scientists. W. Nernst, who was nominated in 1911 by Planck, received Chemistry Nobel Prize in 1920. J. Stark received the

Physics Nobel Prize in 1919. A. Einstein, who was nominated thrice by Planck for the general theory of relativity received Physics Nobel Prize in 1921 "for his services to Theoretical Physics, and especially for his discovery of the law of the photoelectric effect" [28].

Between 1923 and 1933, F. Paschen and A. Sommerfeld were nominated eight times by Planck, but without success.

It is well-known that after Nazi Regime came in power, most of scientists of Jews origin were forced to leave Germany. O. Stern was such a case.He was nominated twice by Planck. Stern received the Physics Nobel Prize in 1943 as American citizen. For Indian readers it might be of interested that C.V. Raman on Oct. 25, 1933 wrote a letter to the NC and stressed not only the scientific work, but also the political situation. For instance,

> "I understand, however, that professor Stern has been displaced from his chair by the present Government in Germany. The award of the Nobel Prize to him will have at least this great merit that it would relieve him from distress and enable him to continue his most important investigations" [29].

During the critical political times Planck nominated only foreign scientists or scientists of German origin who had left Germany. His last nomination was in favour of L. Meitner and she was the only woman nominated by him. Then 89 years old Planck, who had suffered much on private level, due to death of his son, who was killed by Nazi regime, practically was too old to write a proper letter of nomination. He wrote just one line saying the Physics Nobel Prize for the year 1947 be awarded to L. Meitner.

From Table 1 we also conclude that Planck nominated 19 scientists. Out of them 15 sooner or later received the Nobel Prize. From the 15 winner, 10 were 'non-German' by nationality. If we include O. Stern, who received NP as American citizen, this number rises to 11. His five nominated German scientists won the Prize.

3 Conclusions

Max Planck who gave the hypothesis of the energy quanta was an integrated part of the international scientific community. During his scientific career, the Nobel Committee almost regularly asked him to send proposals for the Nobel Prizes. He nominated scientists from the USA, Canada, and other European countries like Italy, Switzerland, Austria and Denmark. Out of 19 nominated candidates, 10 were either German of German origin. Only four persons nominated by him did not get the Prize, while the rest fifteen were honoured. This suggests that he was in a position to judge the quality of work of his contemporaries.

The only female scientist nominated by M. Planck was L. Meitner.

Out of 19 nominated candidates E. Rutherford (NP winner 1908) and W. Nernst (NP winner 1920) were awarded Chemistry Nobel Prize by the Swedish Academy of Sciences.

In majority of the cases, Planck nominated those candidates, whose work supported the quantum theory, that is, Planck's idea. His nomination praxis shows – how a scientist directly or indirectly 'forces' his ideas on the scientific community.

Our case study shows that minor corrections are asked for in the standard literature on Nobel Prizes. For instance, in E. Crawford *et al.*, A. Einstein's nomination by Planck in the years 1920 is missing [30]. Similarly, F. Paschen and A. Sommerfeld nomination by Planck, of Jan. 29, 1924, which reached the Nobel Committee on Feb. 4, 1924, escaped the attention of authors [31].

Acknowledgements:

We are thankful to Ms. Maria Asp and Prof. Karl Grandin, History of Science, Royal Swedish Academy of Science, Stockholm for sending us nomination letters, referred to in this article. One of us (RS) thanks Prof. Michael Komorek, Research Group - Physics Didactic and Science Communication, for providing research facilities.

References

1. The information is taken from, Maurmair, Silke/Harders, Levke (2014): Max Planck 1958-1947, in: DeutschesHistorisches Museum LeMO, https://www.dhm.de/lemo/biografie/max-planck (17.01.2021). Nobel Lecture (1967): Max Planck. Biographical, in: The Nobel Prize in Physics, https://www.nobelprize.org/prizes/physics/1918/planck/biographical/ (17.01.2021).
2. J.L. Heilbron, *The Dilemmas of an upright man – Max Planck and the fortunes of German science,* Harvard University Press, Cambridge 2000. H. Roos, A. Hermann, (Ed.), *Max Planck – Vorträge, Reden, Erinnerungen,* Springer Verlag, Berlin (2001).
3. H. Kangro, *Early History of Planck's Radiation Law*, Taylor and Francis, London (1976).
4. E. Crawford, *Isis* **75 (**1984) 503-522. R.M. Friedmann, *Historical Studies in the Natural Sciences***20**, 1989, 63-77. E. Crawford, J.L. Heilbron, R. Ullrich, *The Nobel population* (1901-1937), The Regents of the University of California, California 1987. G. Kueppers, P. Weingart, N. Ulitzk, *Die Nobelpreise in Physik und Chemie* (1901-1929), *Materialien zum Nominierungsprozess*, B.K. Verlag GmbH, Bielefeld (1982). R.M. Friedman, *The politics of excellence: Behind the Nobel Prize in science*, A W.H. Freeman Book, New York 2001. E. Crawford, *Historical studies in the Nobel archives – the prizes in science and medicine*, Universal Academy Press, Inc., Tokyo (2002). E. Crawford, *The beginning of the Nobel Institution – The science prizes* (1901-1915), Cambridge University Press, Cambridge (1981).
5. R. Singh, B. Martens, *Sci. Cult.* **87 (**2021) 171-179.
6. M. Planck to Nobel Committee (abb. NC), Jan. 14, 1901.
7. In 1902, Nobel Prize was shared by H.A. Lorentz and P. Zeeman.
8. M. Planck to NC, telegram, Jan. 31, 1902.
9. M. Planck to NC, Jan. 19, 1902. M. Planck to NC, Jan. 12, 1903. M. Planck to NC, Jan. 125, 1904.
10. M. Planck to NC, Jan. 26, 1905. M. Planck to NC, Jan. 28, 1906.
11. M. Planck to NC, Jan. 26, 1907. M. Planck to NC, Jan. 20, 1908.
12. M. Planck to NC, Jan. 22, 1911.
13. M. Planck to NC, Jan. 8, 1916.
14. M. Planck to NC, Jan. 27, 1919. M. Planck to NC, Jan. 25, 1920. M. Planck to NC, Jan. 22, 1922.
15. M. Planck to NC, Jan. 22, 1922.
16. M. Planck to NC, Jan. 14, 1923. M. Planck to NC, Jan. 29, 1924. M. Planck to NC, Jan. 20, 1925. M. Planck to NC, Jan. 26, 1926. M. Planck to NC, Jan. 22, 1928. M. Planck to NC, Jan. 24, 1929. M. Planck to NC, Jan. 24, 1932. M. Planck to NC, Jan. 14, 1933.
17. In 1927, A.H. Compton shared the NP with C.T.R. Wilson.
18. M. Planck to NC, Jan. 1, 1927.
19. M. Planck to NC, Jan. 1, 1929.
20. M. Planck to NC, Jan. 1, 1929.
21. M. Planck to NC, Jan. 2, 1931.

22. M. Planck to NC, Jan. 15, 1934.
23. M. Planck to NC, Jan. 1, 1935.
24. In 1936, C.D. Anderson shared the NP with V. Hess.
25. M. Planck to NC, Jan. 22, 1936.
26. M. Planck to NC, Jan. 17, 1937.
27. M. Planck to NC, Jan. 14, 1947.
28. https://www.nobelprize.org/prizes/physics/1921/summary/, Feb. 9, 2021. For more detail, see A. Elzinga, *Einstein's Nobel Prize – A glimpse behind closed doors – The archival evidence*, Science History Publications/USA, Sagamore Beach (2006).
29. For more detail, see R. Singh, *Chemistry and Physics Nobel Prizes – India's contribution*, Shaker Publisher, Aachen (2016) pp. 61-88.
30. See under Ref. 4, E. Crawford et al. (1987) pp. 81-82.
31. Ibid., E. Crawford et al. (1987) pp. 95-96.

Scientific Voyage
Vol. 2, No. 3,
Page 34-34 (2021)

SCIENTIFIC VOYAGE
ISSN: 2395-5546

GCECT
Publication
July - Sept.

OBITUARY

Thanu Padmanabhan

(10 March 1957 – 17 September 2021)

Thanu Padmanabhan was an Indian theoretical physicist and cosmologist whose research spanned a wide variety of topics in gravitation, structure formation in the universe and quantum gravity. He published nearly 300 papers and reviews in international journals and ten books in these areas. He made several contributions related to the analysis and modelling of dark energy in the universe and the interpretation of gravity as an emergent phenomenon. He was a Distinguished Professor at the Inter-University Centre for Astronomy and Astrophysics (IUCAA) at Pune, India. His doctoral advisor was Prof. J.V. Narlikar.

A Stanford study in 2020, listing top scientists in different fields, ranked Padmanabhan as 24th in the world in his research area.

Padma Shri (from the President of India, 2007)

Quotes by Padmanabhan:

"*I worry a lot about putting together the principles of quantum theory and gravity in a consistent manner.''*

"How did structures like galaxies, clusters of galaxies, etc. form? I try to get somewhere in understanding this question though progress has become very difficult in the recent years since this area has become fashionable."